Control of the pH−Dependence of the Band Edges of Si(111) Surfaces Using Mixed Methyl/Allyl Monolayers

ARTICLE *in* THE JOURNAL OF PHYSICAL CHEMISTRY C · APRIL 2011

Impact Factor: 4.77 · DOI: 10.1021/jp109799e

7 AUTHORS, INCLUDING:

Shannon Boettcher
University of Oregon
65 PUBLICATIONS **4,919** CITATIONS

SEE PROFILE

Bruce Brunschwig
California Institute of Technology
202 PUBLICATIONS **7,706** CITATIONS

SEE PROFILE

THE JOURNAL OF PHYSICAL CHEMISTRY C

ARTICLE

pubs.acs.org/JPCC

Control of the pH-Dependence of the Band Edges of Si(111) Surfaces Using Mixed Methyl/Allyl Monolayers

Erik Johansson, Shannon W. Boettcher, Leslie E. O'Leary, Andrey D. Poletayev, Stephen Maldonado, Bruce S. Brunschwig, and Nathan S. Lewis*

Beckman Institute and Kavli Nanoscience Institute, Noyes Laboratory, 127-72 California Institute of Technology, Pasadena, California 91125, United States

ABSTRACT:

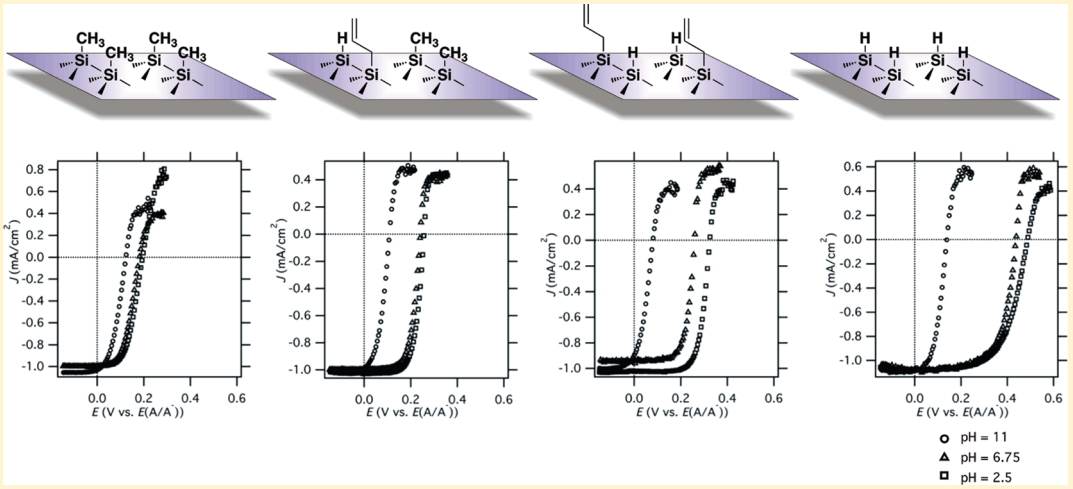

The open-circuit potentials of p-Si/($(MV^{2+}/MV^{+})_{(aq)}$) junctions with Si(111) surfaces functionalized with H−, CH_3−, CH_2CHCH_2−, or mixed CH_3−/CH_2CHCH_2− monolayers have been investigated as the solution pH was changed from 2.5 to 11. The pH sensitivity of the open-circuit potentials, and therefore the band-edge positions, was anticorrelated with the total fraction of Si atop sites that were terminated by Si−C bonds. This behavior is consistent with the hypothesis that the non Si−C terminated atop sites were initially H-terminated and were unstable to oxide growth under aqueous conditions with the oxidation-product inducing a pH-dependent dipole. Metal-semiconductor junctions between Hg and CH_3-, CH_2CHCH_2-, or mixed CH_3-/CH_2CHCH_2-terminated n-Si(111) surfaces formed rectifying Hg/Si Schottky junctions and exhibited mutually similar barrier-heights (∼0.9 V), suggesting similar magnitudes and direction of the surface dipoles on all of these functionalized surfaces.

I. INTRODUCTION

To yield efficient photoelectrochemical energy-conversion systems, the band-edge positions of semiconducting electrodes must be appropriately positioned relative to the redox systems of interest.[1] In many cases, materials that have band gaps that are suitable for use in photoelectrochemical solar energy conversion devices have band-edge positions that are not optimally positioned energetically. For example, the potential of the conduction band edge of n-TiO_2 surfaces is slightly positive of the H_2O/H_2 potential, precluding the use of TiO_2 for efficient photoelectrochemical production of H_2 from water under standard conditions.[2] Similarly, the conduction band-edge potential of n-Fe_2O_3 surfaces is too positive to allow for production of H_2 from H_2O, even if efficient charge separation and collection could be achieved with Fe_2O_3 photoanodes.[2,3] A third example is that the band-edge positions of p-Si photocathodes are too negative to allow for large photovoltages to be obtained for the reduction of H_2O to H_2.[4]

Two related approaches to achieving band-edge control involve band-edge engineering and band gap engineering.[5−7] The band-edges of $GaInP_2$ have been deliberately shifted by modifying the semiconductor surface with thin films of highly insoluble compounds that shifted both the flat-band potential and the onset of photocurrent of the electrodes.[6] Band-gap engineering involves the deliberate modification of a material to produce an absorber that has the appropriate band gap, as is commonly used in tandem solar cells to satisfy the constraint of equal photon absorption from a standard solar spectrum.[8] One way of achieving this is to adjust the band gap of the materials. An example of the efficiency attainable with this technique involves the use of $GaInP_2$ (E_g = 1.83 eV), an alloy of GaP (E_g = 2.26 eV)

Received: October 12, 2010
Revised: February 22, 2011
Published: April 08, 2011

Scheme 1. Change in the Energetics at Flat-Band Conditions with Increasing pH for a pH-Sensitive Semiconductor and pH-Insensitive Redox Couple (| → ||) and for Both a pH Sensitive Semiconductor and Redox Couple (| → |||)[a]

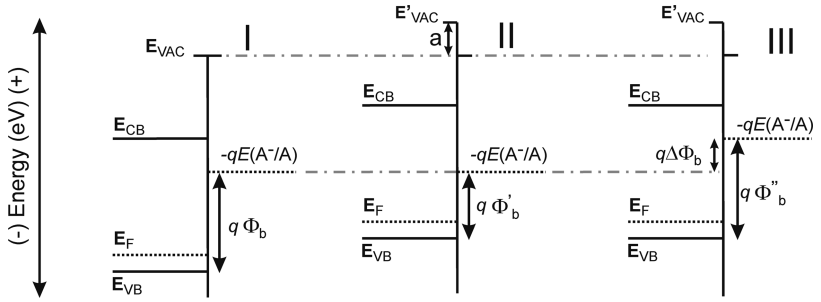

[a] Here *a* represents the change in energy of passing an electron across an interfacial dipole. There is no effect observed on the interfacial energetics if both the solution redox couple and the interfacial dipole exhibit the same dependence on the solution pH; the barrier height ($q\Phi_b = q\Phi_b''$) remains constant (| → |||) as the pH is increased. The barrier height will change with pH for a semiconductor/liquid junction between a pH-insensitive redox couple and pH-sensitive semiconductor (||) or for a pH-sensitive redox couple and pH-insensitive semiconductor. In this later case, the barrier-height can be expressed as $q\Phi_b'' = q\Phi_b + q\Delta\Phi_b$. $\mathbf{E}_{VAC}$ is the vacuum energy; $\mathbf{E}_{CB}$ is the conduction band energy; $\mathbf{E}_{VB}$ is the valence band energy; $-qE(A/A^-)$ is the solution redox energy; $\mathbf{E}_F$ is the Si Fermi-energy.

and InP ($\mathbf{E}_g$ = 1.35 eV), together with GaAs, to produce a 12.4% efficient tandem cell for photoelectrochemical water splitting.[5] $GaInP_2$ and GaAs are a near-ideal pair of absorbers in that they satisfy the constraint of equal photon absorption from a standard solar spectrum.[8]

Another approach to achieving band-edge control involves changing the pH of the solution. If pH-dependent surface functionalities are present, as the pH is changed the band-edge positions of the semiconductor photoelectrode will shift relative to a fixed reference potential.[9] This approach is useful for manipulating the barrier heights of semiconductor surfaces in contact with pH-independent aqueous redox species, such as methyl viologen$^{2+/+}$, $MV^{2+/+}$, or $[Co(2,2'\text{-bipyridyl})_3]^{3+/2+}$ in H_2O. A pH-dependent shift of the band-edge energies is expected for metal oxide electrodes in contact with aqueous solutions, due to the protonation/deprotonation of surface OH-species, as observed for many metal oxides, including ZnO.[10] The ability to control the band-edge energies of n-ZnO by varying the solution pH was used to investigate the driving-force dependence of interfacial charge-transfer reactions at the n-ZnO/H_2O interface, in contact with an aqueous solutions containing redox couples having pH-independent redox potentials.[10] The driving force was manipulated by changing the solution pH, because the n-ZnO band-edge positions were shifted relative to the pH-independent redox potential of the solution redox couple.[10] Such surfaces, however, do not show a change in energetics in contact with pH-dependent aqueous redox systems, such as the half-reactions involved with the oxidation or reduction of H_2O (Scheme 1a), because the H_2O/H_2 and O_2/H_2O redox potentials are also pH-dependent. In this case, any Nernstian (59 mV/pH-unit) shift in the band-edge potentials as a function of pH is canceled by a concomitant Nernstian shift in the redox potential of the solution redox species, leaving the relative interfacial energetics of the system unchanged.

When the redox couple of interest has a pH-dependent redox potential, an alternative approach to achieving band-edge control, and thus control of the interfacial energetics of the semiconductor/liquid interface, is required. Functionalization of the semiconductor surface in a fashion that eliminates pH-dependent surface sites allows for a concomitant change in the barrier height at the semiconductor/liquid interface (Scheme 1b) for pH-dependent half reactions in contact with such surfaces. Surface

Scheme 2. Possible Introduction of a Controllable, Fixed Interfacial Dipole by Surface Functionalization Allowing Manipulation of the Band-Edge Positions Relative to a Fixed Reference Potential[a]

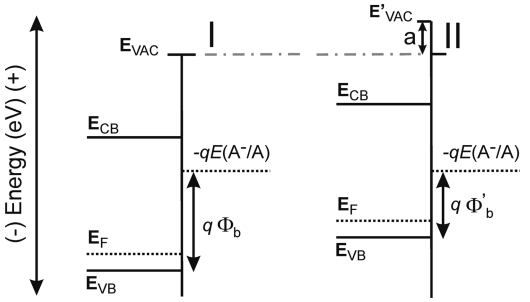

[a] $\mathbf{E}_{VAC}$ is the vacuum energy; $\mathbf{E}_{CB}$ is the conduction band energy; $\mathbf{E}_{VB}$ is the valence band energy; $-qE(A/A^-)$ is the solution redox energy; $\mathbf{E}_F$ is the Si Fermi-energy.

functionalization can also introduce a controllable, fixed interfacial dipole to allow manipulation of the band-edge positions relative to a fixed reference potential (band-edge engineering, Scheme 2). Provided that such surface functionalization can be performed in a fashion that allows for facile interfacial transfer of minority charge carriers with minimal surface recombination losses, control over the barrier height of such photoelectrodes can provide an approach to optimization of the performance of such photoelectrodes in half reactions of relevance to production of fuels, such as water splitting using sunlight. This is possible only if the semiconductor surface is free of electronic defects, which will otherwise limit the performance of such photoelectrodes.

Herein we explore the possibility of controlling the pH-dependent band-edge positions of single crystal p-Si photocathodes. The valence band-edge potential of Si is displaced by only ~0.3 V from the H_2O/H_2 formal potential, $E^{o\prime}(H_2O/H_2)$, severely limiting the photovoltage, and thus the energy conversion efficiency that can be obtained from such interfaces. Because the solution redox potentials and the band-edge positions are both pH-dependent, pH control is precluded as a means of manipulating the energetics of the Si/H_2O interface.[11−14] Hence although incorporation of effective catalysts could improve the fill factor of Si photocathodes,

dx.doi.org/10.1021/jp109799e |J. Phys. Chem. C 2011, 115, 8594–8601

low photovoltages are expected unless the band-edge positions of the Si can be manipulated relative to $E^{o\prime}(H_2O/H_2)$.

Organic molecules have been attached to Si surfaces using numerous techniques.[15−18] The reasons for such Si surface functionalization include passivation toward oxidation,[17] achieving low interfacial trap densities,[19] control over band energetics,[20,21] and introduction of functional groups for further chemistry and sensing applications.[22] Methylation of Si(111) surfaces provides improved oxidation resistance,[16] a low electronic surface defect density,[19,23] an essentially complete coverage of Si(111) atop sites,[24] and a small barrier to electron tunneling.[25] A recent study demonstrated that the pH-dependence of the band-edge positions of an n-Si(111) electrode could be suppressed efficiently by methylating the surface using a two-step halogenation/alkylation process.[26]

Methylated Si surfaces do not however provide a suitable surface for further chemical functionalization, because the CH_3- group itself is highly inert. To address this issue, Si(111) surfaces have been passivated using $CH_2{=}CHCH_2-$ groups.[27] However, such surfaces show less than complete coverage of Si atop sites, as well as lesser oxidation resistance and higher electronic defect densities than CH_3-Si(111) surfaces.[27,28] Accordingly, mixed CH_3-/CH_2CHCH_2- monolayer-protected Si(111) surfaces (MM-Si(111)) have been investigated to maintain the passivation properties of the CH_3-Si(111) surface, while introducing functional groups for secondary chemistry. X-ray photoelectron spectroscopy (XPS), grazing angle attenuated total reflectance Fourier-transform infrared (GATR-FTIR) spectroscopy, transmission FTIR, and surface recombination velocity (S) measurements have indicated that that the oxidation resistance, total coverage, and electronic defect density of such surfaces are superior to that of CH_2CHCH_2-Si(111) surfaces.[28] In this work, we have evaluated the dependence of the open-circuit potential on pH of CH_3-, CH_2CHCH_2-, and MM-terminated Si(111) photocathodes when in contact with an aqueous solution that contains a pH-independent redox-couple. The ability to efficiently suppress the pH-dependence of the Si band edges opens up the possibility to optimize the performance of Si photocathodes as outlined above (Scheme 1), by changing the pH of the solution. It is especially important to suppress the pH dependence for surfaces having functional moieties such as CH_2CHCH_2- groups, because such functional groups can be used to attach with direct electrical contact, molecular catalysts to the Si surface. We have also studied the interfacial dipoles that are introduced by CH_3-, CH_2CHCH_2-, and MM-termination of Si(111) surfaces. Because of poor band-edge alignment, low photovoltages, and thus low energy-conversion efficiencies, are expected for Si photocathodes that are used for water reduction/hydrogen production. Successful band-edge control could be used to shift both the flat-band potential and the onset of photocurrent, thus increasing the energy-conversion efficiency of such systems.

II. EXPERIMENTAL SECTION

A. Materials. All chemicals were used as received. Water was obtained from a Barnstead Nanopure system and had a resistivity of ≥18.2 MΩ cm. Methyl viologen ($MV^{2+/+}$) dicholoride (Aldrich) was used as received. The Czochralski grown Si(111) wafers used for photoelectrochemical measurements (Silicon Quest International, Santa Clara, CA) were p-type doped with B to a resistivity of 1−2 Ω cm and were 500−550 μm thick. Wafers used for differential capacitance versus voltage ($C^{-2}-V$) measurements (Crysteco Inc.) were As-doped n-type to a resistivity of 2.60 ± 0.05 Ω cm (as measured using a four-point probe setup) and had a thickness of 475−500 μm. Wafers used for surface recombination velocity measurements (TOPSIL) were double-side polished with a thickness of 350 ± 25 μm and had a resistivity of 4000−8000 Ω cm.

B. Functionalization of Si(111) Surfaces. CH_3-Si(111), CH_2CHCH_2-Si(111), and MM-Si(111) surfaces were synthesized as described previously.[28] The controlled and reproducible synthesis of functionalized Si(111) surfaces was performed as described below.

1. Cleaning of Si(111) Surfaces. After rinsing sequentially with H_2O, methanol, acetone, methanol, and H_2O, the Si(111) samples (4 cm × 1 cm) were immersed into freshly made piranha solution (1:3 by volume of 10.1 M H_2O_2(aq)/18 M H_2SO_4) and heated to 100 °C for 5 min. After the piranha treatment, the wafers were slowly cooled to room temperature and were rinsed with water. The samples were not allowed to dry during the cleaning procedure or prior to the hydrogen-termination steps.

2. Hydrogen-Termination of Si(111) Surfaces. Directly after the cleaning procedure, the Si(111) samples were etched in 6 M HF(aq) (prepared by diluting 49% HF(aq), obtained as semiconductor grade from Transene Company, Inc., Danvers, MA)), to remove the silicon oxide. Following a brief H_2O rinse, the samples were etched for 10 min in 11 M NH_4F(aq) (semiconductor grade, Transene Company, Inc., Danvers, MA) that had been purged with Ar for at least 45 min. The NH_4F(aq) was continuously purged during the etching process, and the samples were agitated to prevent bubble accumulation on the wafer surface. This process produced atomically flat Si(111), as indicated by transmission infrared spectroscopy.[29] Immediately after etching, the samples were introduced into a N_2(g)-purged flush-box that contained less than 10 ppm O_2.

3. Chlorine-Termination of Si(111) Surfaces. To chlorinate the surfaces, the H-terminated Si(111) surfaces were immersed into a saturated solution of PCl_5 (99.998% metal basis, Alfa Aesar) in chlorobenzene (Anhydrous, 99.8%, Sigma Aldrich), to which a small amount of benzoyl peroxide (Aldrich reagent grade, 97%, Sigma Aldrich), acting as a radical initiator, had been added. The solution was heated to 90−95 °C for 45 min, after which the sample was rinsed with chlorobenzene (99.8%, anhydrous, Aldrich) followed by tetrahydrofuran (99.9%, anhydrous, inhibitor free, Aldrich) (THF).

4. Alkylation of Si(111) Surfaces. Cl-Si(111) samples were immersed at 70−75 °C for 3 h in an alkylating solution that contained 1.0 M of either CH_3MgCl (diluted from 3.0 M CH_3MgCl in THF, Aldrich), CH_2CHCH_2MgCl (diluted from 2.0 M CH_2CHCH_2MgCl in THF, Aldrich), or a mixture CH_3MgCl and CH_2CHCH_2MgCl (2 mol % CH_2CHCH_2MgCl and 98 mol % CH_3MgCl). The samples were then rinsed THF and sonicated in CH_3OH, CH_3CN, and then H_2O. The alkylated Si(111) samples were stored under N_2(g) until use.

C. Photoelectrochemical Measurements. *1. Electrode Fabrication.* p-Si(111) samples were sectioned into squares having an area of ∼1 × 1 cm^2 and were cleaned using H_2O, methanol, acetone, methanol, and then H_2O. To make ohmic contact to the back of the wafer, the Si sample was scribed with a diamond-tipped pen dipped in In−Ga eutectic, thus ensuring that the eutectic contacted freshly exposed Si. Tinned Cu wire was contacted to the In−Ga eutectic and was secured into place using conductive Ag print. Additional mechanical stability was ensured by further securing the wire to the back of the wafer using epoxy (Hysol 1C, McMaster-Carr), while ensuring that the epoxy did not contact the front of the wafer. The tinned copper

wire was threaded through a 7 mm outer-diameter glass tube, after which the wafer was sealed to the glass tube using Apiezon type W wax (SPI supplies, West Chester, PA). Finally, an area of ~0.1 cm^2 was defined using black nail polish. The exact area was determined for each sample (Epson scanner, ImageJ 1.41) so that accurate current densities could be established.

2. Solutions. Solutions of three different pH values were used to evaluate the dependence of the open circuit voltage, V_{oc}, on pH. Phthalte (pH = 2.5) and phosphate (pH = 6.75 and pH = 11.0) buffers were prepared according to literature methods.[30] The ionic strength of the solutions was adjusted to 1.0 M by addition of KCl. The pH of the solutions was measured using a VWR Scientific model 8010 pH meter. Prior to any electrochemical experiments, all solutions were purged with Ar for a minimum of 30 min.

Bulk electrolysis was used to prepare solutions that had well-defined and stable redox potentials. Carbon cloth was used as the working electrode, and a platinum mesh counter electrode was separated from the main compartment by a medium porosity glass frit. The oxidized MV^{2+} redox species, 0.010 M of $(MV^{2+})(Cl^-)_2$, was reduced at an applied bias of −0.7 versus a saturated calomel electrode (SCE) until the solution potential reached a value of −0.65 V versus SCE.

3. Current Density versus Potential Measurements. Photoelectrochemical measurements were carried out in a cylindrical, flat-bottomed, three-neck flask that contained ~25 mL of solution that had been purged for a minimum of 30 min and then maintained under a continuous flow of Ar. The three-electrode setup consisted of a magnetic stir bar, a saturated calomel electrode (SCE) reference, a large carbon-cloth counter electrode (~10 cm^2), and a Si(111) working electrode. All data were collected relative to SCE.

Current density versus potential ($J-E$) data were obtained at a scan rate of 0.010 V s^{-1} with a Solartron model SI 1287 potentiostat controlled by CorrWare software. Before and after each data collection run, the solution potential versus SCE was measured using a carbon-cloth electrode, so that the $J-V$ data could be displayed as current density versus the Nernstian potential of the solution, $E(A/A^-)$. Illumination was provided by a tungsten−halogen lamp equipped with a collimator and a frosted-glass diffuser. The separation between the sample and the light-source was adjusted such that the light-limited cathodic current density was 1 mA cm^{-2}.

D. Differential Capacitance Measurements. The ~4 cm × 1 cm n-Si(111) samples were diced and cleaned as described above. To make an ohmic contact, the back of the wafer was scribed with a diamond-tipped pen dipped in In−Ga eutectic, thus ensuring that the eutectic contacted freshly exposed Si. The sample was then placed onto a freshly polished Cu plate, providing a convenient ohmic back contact. A Kalrez O-ring was then placed on top of the wafer, and a small amount of Hg (Electronic grade, 99.9998% (metals basis), Alfa Aesar) was poured into the area defined by the O-ring. The Hg-contact had an area of 0.118 cm^2 (Epson scanner, ImageJ 1.41), and the Hg itself was contacted using a Pt wire, because Pt is known not to amalgamate. Impedance measurements were obtained with a Schlumberger Model SI 1260 frequency response analyzer controlled by ZPlot for Windows (v. 2.6).

E. Surface Recombination Velocity Measurements. *1. Sample Preparation.* H-terminated nearly intrinsic Si(111) samples (~1 cm × 1 cm) were prepared by etching for 45 s in 6 M HF(aq). The samples were then immediately transferred to a shallow Petri dish that contained a buffer solution (phthalte (pH = 2.50) or phosphate (pH = 11.00)) that had been purged with Ar for a minimum of 30 min. The Petri dish was immediately sealed with parafilm. The samples were transported to the contactless microwave conductivity setup and lifetimes were measured once every minute for 5 min.

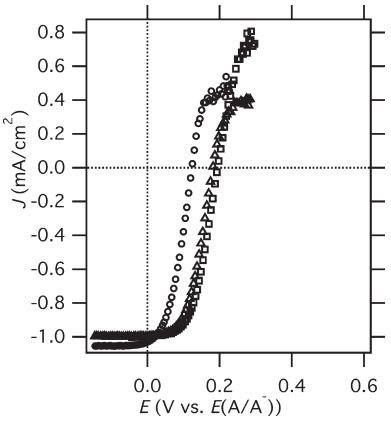

Figure 1. $J-V$ data obtained for CH_3-p-Si(111)/(MV^{2+}/MV^+). Increasing pH resulted in a decrease in V_{oc}. The symbols ○, Δ, and □ signify a solution pH of 11, 6.75, and 2.5 respectively.

2. Carrier Lifetime Measurements. The carrier lifetimes were measured by observing the photoconductivity decay. Measurements were made using a contactless microwave conductivity apparatus.[27,28,31] A 20 ns laser pulse (905 nm, OSRAM laser diode and ETX-10A-93 driver) generated the excess charge carriers in the sample. The concentration of charge carriers as a function of time was monitored using reflected microwave radiation, detected by a PIN diode. Carrier lifetimes were extracted by fitting the obtained data to an exponential curve, and the data were then converted to S values using known relationships.[27]

III. RESULTS

A. Photoelectrochemical Measurements. Figures 1−4 display representative $J-E$ data for CH_3-, MM-, CH_2CHCH_2- and H-terminated p-Si(111) photoelectrodes, respectively, in solutions having pH values of 2.50, 6.75, or 11.0. The photocurrent was adjusted such that the limiting photocurrent density for all samples was within 15% of 1.0 mA cm^{-2}. Furthermore, the photocurrent density for any electrode, measured in solutions of different pH, varied by less than 15%. Ideally, the dependence of V_{oc} on photocurrent, and thus on light intensity, is described by eq 1

$$V_{oc} \cong \left| \frac{AkT}{q} \ln\left(\frac{J_{ph}}{J_0}\right) \right| \quad (1)$$

where A is the diode quality factor (ideally 1.0), k is the Boltzmann constant, T is the temperature, q is the unsigned elementary charge, J_{ph} is the photocurrent density and J_0 is the exchange current density. A 15% difference in J_{ph} would therefore produce a 4 mV difference in the open-circuit voltage.

The open-circuit voltage, obtained from the $J-E$ data by measurement of the voltage at which no current flowed, was observed to depend on the solution pH (Figures 1−4, Table 1). Because the redox potential of $MV^{2+/+}$ is independent of pH,[26] the observed shift in V_{oc} is due to changes at the semiconductor

dx.doi.org/10.1021/jp109799e |J. Phys. Chem. C 2011, 115, 8594–8601

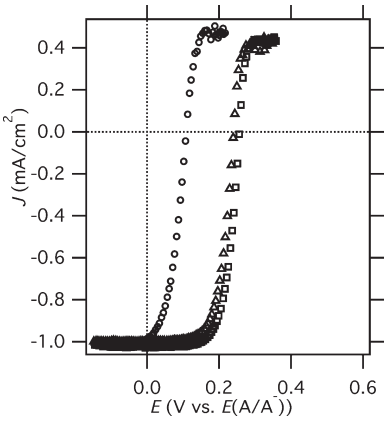

Figure 2. $J-V$ data obtained for MM-p-Si(111)/(MV^{2+}/MV^{+}). Increasing pH resulted in a decrease in V_{oc}. The symbols ○, Δ, and □ signify a solution pH of 11, 6.75, and 2.5 respectively.

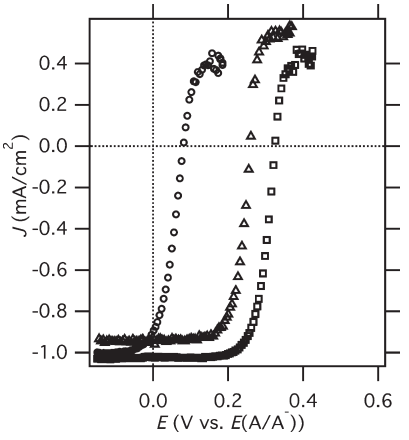

Figure 3. $J-V$ data obtained for CH_2CHCH_2-p-Si(111)/(MV^{2+}/MV^{+}). Increasing pH resulted in a decrease in V_{oc}. The symbols ○, Δ, and □ signify a solution pH of 11, 6.75, and 2.5 respectively.

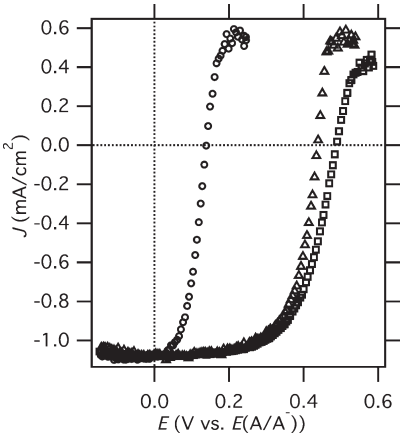

Figure 4. $J-V$ data obtained for H-p-Si(111)/(MV^{2+}/MV^{+}). Increasing pH resulted in a decrease in V_{oc}. The symbols ○, Δ, and □ signify a solution pH of 11, 6.75, and 2.5 respectively.

electrode. Over a pH range of 8.5 units (from pH 2.50 to pH 11.00), the V_{oc} shifted on average by −9, −17, −28, and −42 mV/pH-unit for CH_3-, mixed CH_3-/CH_2CHCH_2-, CH_2CHCH_2-, and H-terminated Si(111) photocathodes, respectively, with the pH-dependence of the open-circuit voltage clearly increasing as the surface functionalization was changed from CH_3- to MM- to CH_2CHCH_2- to H-termination. For all surfaces, the pH dependence of V_{oc} was a function of the absolute pH of the solution, being greater at high pH values than at low pH values. The measured values of −9, −17, −28, and −42 mV/pH-unit for CH_3-, mixed CH_3-/CH_2CHCH_2-, CH_2CHCH_2-, and H-terminated Si(111) photocathodes, respectively, represent the average values over the entire pH-range of 8.5 units (from pH 2.50 to pH 11.00).

Table 1. Dependence of V_{oc} on Solution pH for R-Si(111) Electrodes in Aqueous Solutions

	$\Delta V_{oc}/\Delta$pH	
R−	mean (mV/pH unit)	95% confidence interval (mV/pH unit)
CH_3−	−9	±2
MM−	−17	±1
CH_2CHCH_2−	−28	±1
H−	−42	±2

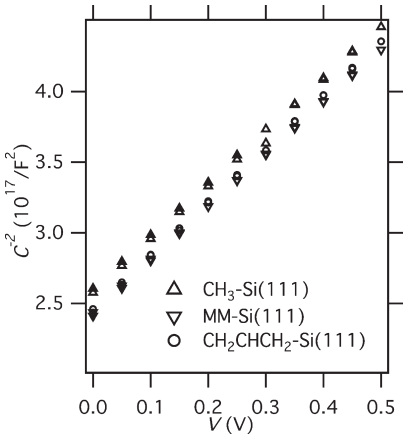

Figure 5. Mott−Schottky ($C^{-2}-V$) plots for various Hg/n-Si(111) junctions.

B. Differential Capacitance Measurements. Figure 5 depicts representative Mott−Schottky plots for Hg/n-Si(111) junctions formed from either CH_3-, MM-, or CH_2CHCH_2-terminated n-Si(111) surfaces. The differential capacitance, C_{diff}, was extracted by fitting the frequency-dependent impedance data to a simple test circuit that consisted of a resistor in series with a parallel capacitor and resistor. Bode plots of the log of the magnitude of the impedance versus frequency showed linear behavior with a slope of unity over a large frequency range, validating the use of the simplified equivalent circuit.

The semiconductor dopant density and the built-in voltage, V_{bi}, of Si for Hg/n-Si junctions were obtained from Mott−Schottky plots by use of eq 2

$$\frac{1}{C_{diff}^2} = \frac{2}{q\varepsilon\varepsilon_0 N_D A_s^2}\left(V + V_{bi} - \frac{k_B T}{q}\right) \qquad (2)$$

where ε and ε_0 are the dielectric constant of Si and the permittivity of vacuum, respectively, N_D is the dopant density, A_s is the junction area, and V_{bi} is the built-in voltage of the

Table 2. Barrier Heights for Hg/n-Si junctions formed with R-Si(111)

R−	V_{bi} (V)	Φ_b (V)	95% confidence interval (V)
CH_3−	0.69	0.94	±0.06
MM−	0.68	0.92	±0.02
CH_2CHCH_2−	0.64	0.89	±0.12

Hg/n-Si junction. All junctions were largely defect-free, as shown by the dopant densities calculated from Mott−Schottky plots and by the values obtained from four-point probe measurements. The values of the dopant density calculated from the slope of the Mott−Schottky plots were in good agreement (less than 25% difference for all samples) with the dopant densities determined independently from four-point probe measurements. Built-in voltages were converted to barrier heights using eq 3

$$\Phi_b = V_{bi} - \frac{k_B T}{q} \ln\left(\frac{N_D}{N_C}\right) \quad (3)$$

where N_C is the effective density of states in the conduction band of Si (2.8×10^{19} cm^{-3}).[32] The measured barrier heights for the Hg/n-Si junctions were ~0.9 V, with no statistical difference observed between the barrier heights of the different types of alkylated Si(111) surfaces (Table 2).

C. Surface Recombination Velocities. Figure 6 displays the surface recombination velocities for H-Si(111) in contact with buffered solutions of pH 2.50 or 11.00. Carrier lifetimes were measured five times for each sample with 1 min intervals during which the samples were not agitated. Values of S < 300 cm s^{-1} were observed for samples in the acidic, pH 2.50, solution, and the S values were observed to increase slowly during the 5 min time period. The S values for samples in the basic, pH 11.0, solution were <25 cm s^{-1}, and S was steady throughout the 5 min time period. Only slow, gradual changes in carrier lifetimes were observed during the 5 min time period for any samples.

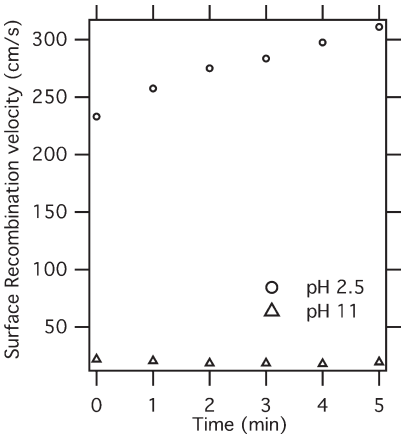

Figure 6. Surface recombination velocities measured for H-Si(111) in basic (pH 11) and acidic (pH 2.5) solutions. Measurements were taken at regular intervals to ensure that the system displayed reasonable stability.

IV. DISCUSSION

A. pH Dependence of V_{oc} for Si(111) Surfaces Terminated by Mixed Methyl/Allyl Monolayers. The minimal pH-dependence of V_{oc} for CH_3-terminated p-Si(111)/$MV^{2+/+}$ contacts (Figure 1) is consistent with expectations for a system in which the flat-band potential of the photoelectrode is largely independent of pH. Prior measurements of the dark, forward biased $J-E$ behavior of CH_3-terminated n-Si(111) surfaces in buffered (pH 1.4 to 11.0) aqueous solutions that contained 10 mM MV^{2+} displayed a minimal pH dependence of E_{fb} and are thus in agreement with the results presented herein for p-Si photocathodes.[26] This behavior is consistent with expectations for a surface in which atop Si atoms are essentially fully terminated by a chemically inert Si−C linkage, thus rendering the energetics of such surfaces insensitive to changes in pH. In contrast, the CH_2CHCH_2-terminated p-Si(111) surfaces (Figure 3) showed a significant dependence of V_{oc} on pH. Due to steric constraints, CH_2CHCH_2− groups can not terminate every Si atop site with Si−C bonds on an unreconstructed Si(111) surface. Consistently, XPS and IR studies have shown that functionalization of Si(111) with CH_2CHCH_2− groups terminates ~80% of the surface Si atop sites with Si−C bonds.[28] Detailed IR spectroscopic studies of ethyl-terminated Si surfaces have revealed that the Si atop sites that are not terminated with Si−C bonds are predominantly terminated by Si−H bonds that result from transfer of beta hydrogens on the ethyl group to surface Si atoms during the Grignard reaction step of the two-step chlorination/alkylation process.[33] Similar behavior is expected for CH_2CHCH_2− termination, leaving some significant fraction of the Si surface terminated by Si−H bonds. In the presence of even mild oxidants, such as MV^{2+}, these Si−H bonds are oxidatively susceptible and can produce Si−OH and subsurface Si-oxide species, thereby introducing a mechanism for obtaining a pH dependence of E_{fb} for such surfaces, in accord with the observed change in V_{oc} with pH for such systems. The mixed monolayer systems, however, allow for nearly complete termination of surface Si atop sites by Si−C bonding. MM-Si(111) surfaces have been shown to contain both allyl and methyl groups and to have a higher Si−C coverage than CH_2CHCH_2-Si(111) surfaces. Such surfaces thus provide an accessible functional group for secondary reactions, such as polymerizations and metal binding, but, as shown in Figure 2, retain the minimal pH dependence that is characteristic of CH_3-terminated Si(111) surfaces. It is reasonable to assume that introduction of Si−O and Si−O−Si bonds will affect the reactivity of Si surfaces. The data presented herein do not allow decoupling of the effects of surface and subsurface oxide-species on the pH stability of the band-edges, and the long-term stability of such surfaces has not been investigated.

The classical model for insulators and nondegenerate semiconductor electrodes predicts that adsorption of a charged species (a proton, for example) will be accompanied by an accumulation of charge at the outer Helmholtz plane:

$$\text{Surface-A} + H^+ \rightleftharpoons \text{Surface-AH}^+$$

The Helmholtz double-layer voltage, that is, the difference in potential between the solid surface and the outer Helmholtz plane, is then predicted to have a Nernstian dependence on pH.[34] However, the chemical activity of the equilibrium species is likely to be a function of surface coverage consistent with observed pH-dependences of the interfacial dipole of <59 mV/pH-unit.[35] For H-terminated Si in contact with aqueous solutions, the pH dependence of the band edges has been reported to range from linear (non-Nernstian),[11] to nonlinear,[12] to Nernstian.[13] The behavior of silica is informative because active surface groups on silica are Si−OH_2^+, Si−OH, and Si−O^-. The lowest

dx.doi.org/10.1021/jp109799e |J. Phys. Chem. C 2011, 115, 8594–8601

concentration of charged species at the surface is expected at the pH for which the silica is not charged, $pH_{pzc} \sim 2$.[20,36] The SiO_2 surface is terminated by an appreciable net surface charge-carrying species that is likely responsible for the interfacial dipole only when the pH of a solution contacting SiO_2 is sufficiently different from pH_{pzc}.[20,37]

For Si(111) surfaces that have been functionalized with dodecyl chains using hydrosilylation chemistry, the band-edge positions have been observed to be dependent on pH. For such surfaces, the flat-band potential varied by −25 mV/pH unit over the pH range 4−7, as determined by differential capacitance measurements.[20] The trend exhibited by all surfaces investigated herein, with a pH dependence primarily observed in neutral to basic conditions, is consistent with expectations that the surface species is Si−OH, which can be deprotonated at higher pH to yield Si−O^-. Si(111) surfaces passivated by decyl, carboxydecyl, or mixed decyl/carboxydecyl monolayers attached via hydrosilylation chemistry, and CH_3− groups attached using anodic decomposition of CH_3MgI, have been investigated using surface photovoltage, photoluminescence, capacitance, and FTIR measurements. Differences in experimental conditions (most notably the presence of dissolved oxygen in the solutions) preclude a more direct comparison to the data presented herein, but consistent agreement exists that the surfaces with lower Si−C coverage exhibit increased pH-sensitivity of the electronic properties of the resulting Si/solution junctions.[38]

The open-circuit voltage is related to the barrier height of the semiconductor/liquid contact, but is also a function of surface- and bulk-recombination processes, and interfacial electron-transfer rates; hence, V_{oc} is an indirect measure of the barrier height. High-quality Si wafers of nominally identical quality and doping density were used for the photoelectrochemical studies, ensuring that the bulk recombination velocity did not affect changes in V_{oc}. The surface recombination velocities of CH_3-, MM-, CH_2CHCH_2-, and H-Si(111) surfaces are similar to each other and are <100 cm s^{-1}.[28] Accordingly, the electronic defect densities have been estimated to range from 1 in 40 000 000 to 1 in 100 000 effective surface recombination sites for H- and CH_2CHCH_2-terminated Si(111), respectively, with CH_3- and MM-terminated surfaces having S values between these extremes.[27,28,39] Hence, the surface recombination velocities of such systems are sufficiently low to not significantly affect the performance in typical device applications. The surface recombination velocity of H-Si(111) immersed in buffered solutions (pH 2.50 and 11.0) was determined to ensure that interactions with the buffer did not result in high S values in the absence of inert Si−C termination. The surface recombination velocity was only weakly dependent on pH for H-Si(111) and was low enough that it would not significantly affect V_{oc}. Hence, the shift in V_{oc} as a function of pH cannot be consistently ascribed to changes in surface-state density.

It has been shown previously that the total coverage (defined as the fraction of Si atop sites terminated by a Si−C bond), surface recombination velocity, and rate of oxidation under ambient conditions are all correlated, and that the surface recombination velocity, and rate of oxidation, increase monotonically with decreasing total coverage.[28] We have demonstrated that this is also valid for the pH dependence of the V_{oc} of the surfaces and systems described above.

The open-circuit potential is also dependent on the electron-transfer rates, which themselves depend on the energetics of the semiconductor/liquid junction. The dependence of the interfacial electron-transfer rates on the interfacial energetics has been investigated in detail previously.[40] Nevertheless, the open-circuit potential is monotonically related to the interfacial energetics, and a decrease in the pH-dependence of the open-circuit potential is therefore related to a decrease in the pH-dependence of the band-edge positions.

B. The Effects of Permanent Surface Dipoles on V_{oc}. A change in the surface dipole for the various functionalized Si(111) systems could also produce different values of V_{oc} for each system. The CH_3− group has been shown to induce a surface dipole of −0.4 eV, as measured by XPS at the BESSY II synchrotron facility in Berlin.[41] Similarly, the ethyl group has been shown to induce a surface dipole of −0.23 eV on Si(111).[42] Previous measurements of the barrier height of Hg/Si junctions in which the Si surface was functionalized with a variety of alkyl-chains, ranging in length from CH_3− groups to octyl-decane chains, has indicated that the barrier height is independent of the chain-length of the alkyl group. These results suggest that the CH_3−, CH_2CHCH_2−, and MM surface moieties used herein all introduce a mutually similar surface dipole.[43,44] While the photocathode data were obtained using p-Si, all Mott−Schottky data in this study were collected using n-Si, because alkyl-terminated p-Si forms very low barrier height junctions with Hg due to the alignment of the respective Fermi levels of Si and Hg, thus precluding Mott−Schottky analysis.[43] The impedance data are consistent with the expectation that the CH_3-, MM-, and CH_2CHCH_2-terminated n-Si(111) surfaces all have surface dipoles of similar magnitude and direction.[42] Interfacial dipole-values extracted from the Mott−Schottky measurements do not and should not be expected to coincide with differences in V_{oc} as a function of surface functionality. The Mott−Schottky measurements yield the geometric average of the surface dipole, while V_{oc} measurements are more sensitive to regions of lower barrier-height. Furthermore, the V_{oc} measurements yield the photovoltage under a certain set of experimental conditions that are much different than those used for the Mott−Schottky measurements. The differences observed between these two measurements highlight their complementary nature.

Notably, the surface-dipole introduced by CH_3-, MM-, and CH_2CHCH_2-termination of Si(111) shifts the band edges to more negative potentials than those observed for the H-Si(111) surface. This shift produces lower barrier height junctions on p-Si (Scheme 1) in the absence of Fermi-level pinning. Movement of the band-edge potentials more negative with respect to a fixed solution redox potential, by introduction of a permanent interfacial dipole, decreases the barrier height for p-type electrodes and thus decreases the maximum attainable V_{oc} for such junctions. For H_2O reduction to H_2, this shift can be overcome by use of a higher solution pH. The band edges are independent of the solution pH due to the permanent interfacial dipole, but the hydrogen reduction potential becomes more negative as the pH of the solution is increased, resulting in a higher barrier height. Alternately, in the case of a regenerative photoelectrochemical cell, a redox couple having a more negative potential could be used to produce a higher barrier-height interface.

V. CONCLUSIONS

H-terminated Si(111) surfaces in contact with $MV^{2+/+}$(aq) displayed a large dependence of the V_{oc} on pH, while CH_2CHCH_2-, MM-, and CH_3-terminated surfaces displayed a consistently smaller pH-dependence. CH_3- and MM-terminated

Si(111) surfaces displayed significantly lower pH dependences than surfaces that were instead functionalized using a hydrosilylation process. The magnitude of the dependence of the band-edge positions on pH correlated with the percentage of Si(111) atop sites that were not terminated by Si−C bonds, suggesting that non Si−C-terminated surface bonds reacted to produce groups, such as Si−OH, that produced the observed pH dependence. CH_3- MM-, and CH_2CHCH_2-termination of Si(111) surfaces all produced similar surface dipoles, as observed using differential capacitance−voltage measurements on functionalized n-Si(111)/Hg contacts. Hence, functionalization can stabilize the band-edge positions of Si in contact with aqueous solutions of varying pH with the degree of stabilization highly dependent on the total Si−C coverage of such functionalized surfaces.

AUTHOR INFORMATION

Corresponding Author

*Phone: (626) 395-6335. Fax: (626) 395-8867 210. Address: E-mail: nslewis@caltech.edu.

ACKNOWLEDGMENT

This work was supported by the National Science Foundation (CHE-0911682) and the Molecular Materials Research Center of the Beckman Institute at the California Institute of Technology. The Kavli Nanoscience Institute (S.W.B) and the Betty and Gordon Moore Foundation (S. M.) are gratefully acknowledged for postdoctoral fellowship support.

REFERENCES

(1) Bard, A. J.; Faulkner, L. R. *Electrochemical methods: fundamentals and applications*, 2nd ed.; John Wiley & Sons, Inc.: New York, 2001.
(2) Nozik, A. J.; Memming, R. *J. Phys. Chem.* **1996**, *100*, 13061–13078.
(3) Xu, Y.; Schoonen, M. A. A. *Am. Mineral.* **2000**, *85*, 543–556.
(4) Tan, M. X.; Laibinis, P. E.; Nguyen, S. T.; Kesselman, J. M.; Stanton, C. E.; Lewis, N. S. *Prog. Inorg. Chem.* **1994**, *41*, 21–144.
(5) Khaselev, O.; Turner, J. A. *Science* **1998**, *280*, 425–427.
(6) Kocha, S. S.; Turner, J. A. *J. Electrochem. Soc.* **1995**, *142*, 2625–2630.
(7) Cohen, R.; Bastide, S.; Cahen, D.; Libman, J.; Shanzer, A.; Rosenwaks, Y. *Adv. Mater.* **1997**, *9*, 746–749.
(8) Bolton, J. R.; Strickler, S. J.; Connolly, J. S. *Nature* **1985**, *316*, 495–500.
(9) Lyon, L. A.; Hupp, J. T. *J. Phys. Chem. B* **1999**, *103*, 4623–4628.
(10) Hamann, T. W.; Gstrein, F.; Brunschwig, B. S.; Lewis, N. S. *Chem. Phys.* **2006**, *326*, 15–23.
(11) Madou, M. J.; Loo, B. H.; Frese, K. W.; Morrison, S. R. *Surf. Sci.* **1981**, *108*, 135–152.
(12) Nakato, Y.; Ueda, T.; Egi, Y.; Tsubomura, H. *J. Electrochem. Soc.* **1987**, *134*, 353–358.
(13) Schlichthorl, G.; Peter, L. M. *J. Electrochem. Soc.* **1994**, *141*, L171–L173.
(14) Harris, L. A.; Wilson, R. H. *Annu. Rev. Mater. Sci.* **1978**, *8*, 99–134.
(15) Allongue, P.; de Villeneuve, C. H.; Cherouvrier, G.; Cortes, R.; Bernard, M. C. *J. Electroanal. Chem.* **2003**, *550*, 161–174.
(16) Bansal, A.; Li, X. L.; Lauermann, I.; Lewis, N. S.; Yi, S. I.; Weinberg, W. H. *J. Am. Chem. Soc.* **1996**, *118*, 7225–7226.
(17) Linford, M. R.; Fenter, P.; Eisenberger, P. M.; Chidsey, C. E. D. *J. Am. Chem. Soc.* **1995**, *117*, 3145–3155.
(18) Teyssot, A.; Fidelis, A.; Fellah, S.; Ozanam, F.; Chazalviel, J. N. *Electrochim. Acta* **2002**, *47*, 2565–2571.
(19) Webb, L. J.; Lewis, N. S. *J. Phys. Chem. B* **2003**, *107*, 5404–5412.
(20) Faber, E. J.; Sparreboom, W.; Groeneveld, W.; de Smet, L.; Bomer, J.; Olthuis, W.; Zuilhof, H.; Sudholter, E. J. R.; Bergveld, P.; van den Berg, A. *ChemPhysChem* **2007**, *8*, 101–112.
(21) Gershewitz, O.; Grinstein, M.; Sukenik, C. N.; Regev, K.; Ghabboun, J.; Cahen, D. *J. Phys. Chem. B* **2004**, *108*, 664–672.
(22) Strother, T.; Cai, W.; Zhao, X. S.; Hamers, R. J.; Smith, L. M. *J. Am. Chem. Soc.* **2000**, *122*, 1205–1209.
(23) Bansal, A.; Li, X. L.; Yi, S. I.; Weinberg, W. H.; Lewis, N. S. *J. Phys. Chem. B* **2001**, *105*, 10266–10277.
(24) Yu, H. B.; Webb, L. J.; Ries, R. S.; Solares, S. D.; Goddard, W. A.; Heath, J. R.; Lewis, N. S. *J. Phys. Chem. B* **2005**, *109*, 671–674.
(25) Maldonado, S.; Lewis, N. S. *J. Electrochem. Soc.* **2009**, *156*, H123–H128.
(26) Hamann, T. W.; Lewis, N. S. *J. Phys. Chem. B* **2006**, *110*, 22291–22294.
(27) Plass, K. E.; Liu, X. L.; Brunschwig, B. S.; Lewis, N. S. *Chem. Mater.* **2008**, *20*, 2228–2233.
(28) O'Leary, L. E.; Johansson, E.; Brunschwig, B. S.; Lewis, N. S. *J. Phys. Chem. B* **2010**, *114*, 14298–14302.
(29) Higashi, G. S.; Chabal, Y. J.; Trucks, G. W.; Raghavachari, K. *App. Phys. Lett.* **1990**, *56*, 656–658.
(30) *CRC Handbook of Chemistry and Physics*, 90th ed.; CRC Press: Boca Raton, FL, 2010.
(31) Forbes, M. D. E.; Lewis, N. S. *J. Am. Chem. Soc.* **1990**, *112*, 3682–3683.
(32) Sze, S. M.; Ng, K. K. *Physics of Semiconductor Devices*, 3rd ed.; Wiley-Interscience: New York, 2007.
(33) Johansson, E.; Hurley, P. T.; Brunschwig, B. S.; Lewis, N. S. *J. Phys. Chem. C* **2009**, *113*, 15239–15245.
(34) Morrison, S. R. *Electrochemistry at Semiconductor and Oxidized Metal Electrodes*; Plenum Press: New York, 1980.
(35) Gerischer, H. *Electrochim. Acta* **1989**, *34*, 1005–1009.
(36) Sverjensky, D. A. *Geochim. Cosmochim. Ac.* **2005**, *69*, 225–257.
(37) Schwarz, J. A.; Driscoll, C. T.; Bhanot, A. K. *J. Colloid Interface Sci.* **1984**, *97*, 55–61.
(38) Aureau, D.; Rappich, J.; Moraillon, A.; Allongue, P.; Ozanam, F.; Chazalviel, J. N. *J. Electroanal. Chem.* **2010**, *646*, 33–42.
(39) Yablonovitch, E.; Allara, D. L.; Chang, C. C.; Gmitter, T.; Bright, T. B. *Phys. Rev. Lett.* **1986**, *57*, 249–252.
(40) Fajardo, A. M.; Lewis, N. S. *J. Phys. Chem. B* **1997**, *101*, 11136–11151.
(41) Hunger, R.; Fritsche, R.; Jaeckel, B.; Jaegermann, W.; Webb, L. J.; Lewis, N. S. *Phys. Rev. B* **2005**, *72*, No. 045317.
(42) Jaeckel, B.; Hunger, R.; Webb, L. J.; Jaegermann, W.; Lewis, N. S. *J. Phys. Chem. C* **2007**, *111*, 18204–18213.
(43) Maldonado, S.; Plass, K. E.; Knapp, D.; Lewis, N. S. *J. Phys. Chem. C* **2007**, *111*, 17690–17699.
(44) Yaffe, O.; Scheres, L.; Puniredd, S. R.; Stein, N.; Biller, A.; Lavan, R. H.; Shpaisman, H.; Zuilhof, H.; Haick, H.; Cahen, D.; Vilan, A. *Nano Lett.* **2009**, *9*, 2390–2394.